ORIGINAL ARTICLE

Evaluation of the Proliferation and Invasion of Human Hepatocellular Carcinoma Cells Subjected to Epirubicin Formulated with Natural Oils in Nanoemulsion

Majidah A. Aljadani[1,2], Mayson H. Alkhatib[1], Sawsan H. Mahassni[1]

[1]Department of Biochemistry, Faculty of Science, King Abdulaziz University, Jeddah, Saudi Arabia, [2]Department of Chemistry, Science and Arts College, Rabigh Campus, King Abdulaziz University, Jeddah, Saudi Arabia

Abstract

Introduction: Nanoformulation provides a promising potential for drug delivery of the chemotherapeutic agents. The current study aimed to solubilize the anticancer drug, epirubicin (EPI), in nanoemulsion consisting of algae (AGA) and cinnamon (CNAM) oils and to evaluate the antitumor activity of the new formula (EPI-AGA-CNAM) on the HepG2 and Huh7 hepatocellular carcinoma (HCC) cells. **Materials and Methods:** The size, surface charge, drug release, anticancer potential, flow cytometric analyses of apoptosis, reactive oxygen species (ROS) generation, and anti-invasion ability were investigated for the new nanoformulations. **Results:** The nanodroplets of EPI-AGA-CNAM, analyzed by the dynamic light scattering, were homogeneously distributed with a mean Z-average diameter and zeta potential of 109.90 ± 2.97 nm and −2.98 ± 0.22, respectively. The enhanced cytotoxicity and apoptotic effect of EPI-AGA-CNAM were observed in HepG2 and Huh7 cell lines as compared to free EPI ($P < 0.001$). The higher amounts of ROS formation in the HCC cells were indicated by the increased sensitivities of the fluorescence DCFH-DA probe in EPI-AGA-CNAM-treated HepG2 and Huh7 cells of 84.56 ± 2.21 and 78.01 ± 3.30, respectively, when compared to those of free EPI-treated cells of 13.6 ± 3.77 and 11.67 ± 4.28, respectively. EPI-AGA-CNAM treatment reduced the invasion ability in both cell lines by about 39%, whereas EPI treatment reduced the invasion ability of HepG2 and Huh7 to 55.58% and 63.35%, respectively. **Conclusion:** EPI-AGA-CNAM-induced apoptosis in HCC cell lines through ROS generation and the inhibition of the invasion ability.

Key words: Apoptosis, drug delivery, essential oils, hepatocellular carcinoma, invasion, reactive oxygen species, Zetasizer

INTRODUCTION

Hepatocellular carcinoma (HCC) is the fifth common cancer in humans and the third leading cause of cancer-related death globally, accounting for approximately 80% of all types of primary liver cancer. The treatment of HCC includes the combination of surgical treatment, cytotoxic chemotherapy, targeted therapy, and radiotherapy. Unfortunately, most of the patients with HCC are not eligible for surgery due to recurrences after resection.[1] Most of the classical chemotherapeutic agents exhibit non-specific targeting by directly damaging the DNA of cancer and healthy cells, which lead to high toxicity. Moreover, resistance to classical chemotherapeutic agents acts as a major problem in cancer therapies.[2] One of the widely used chemotherapeutic agents is epirubicin (EPI), which is an anthracycline used in the treatment of various malignancies and kills cancer cells through various mechanisms.[3,4]

In the past decade, nanotechnology therapy has been predictable as a promising approach to improve therapeutic efficacy and

Address for correspondence:
Mayson H. Alkhatib, Department of Biochemistry, Faculty of Science, King Abdulaziz University, Jeddah, Saudi Arabia. Tel.: +966599240526.
E-mail: mhalkhatib@kau.edu.sa

Received: 02-01-2020
Revised: 01-02-2020
Accepted: 09-02-2020

diminish the side effects associated with cancer treatment.[5] Furthermore, targeted localization to tumors, an active mode of cellular uptake, controlled release drug delivery, more enhanced permeability, and retention effect are associated with nanotechnology therapy.[6] Several EPI formulated nanosystems have been employed including polymeric micelles,[7] gold nanoparticle (GNP),[3] liposomes,[8] carbon nanotube,[9] and poly-lactide-co-glycolic acid nanoparticles.[10]

Nanoemulsion has attracted the attention of researchers in the pharmaceutical and food industries. Nanoemulsion has advantages over conventional drug delivery systems. The main function of nanoemulsion is the delivery of poorly soluble drugs and enhance desirable biodistribution, as well as more reasonable pharmacokinetics and active pharmaceutical compounds to the specific site.[11] Moreover, nanoemulsions may be produced by the inclusion of essential oils, which have beneficial properties such as anticancer, antimicrobial, and anti-inflammatory. Recent studies reported that algae (AGA) and cinnamon (CNAM) oils had potent anticancer activities against various models of cancer *in vitro* and *in vivo* with different tumorigenic and metastatic potential through different mechanisms.[12-14]

With the aim to eliminate the EPI adverse side effects, the current study proposed a new nanoemulsion formulated by mixing Tween 80, Span 20, and the essential oils of AGA and CNAM through using the ultrasonication technique. The anticancer activity of the new formula was evaluated in two types of HCC cells (HepG2 and Huh7).

MATERIALS AND METHODS

Chemicals

EPI was purchased from Ebewe Pharmaceuticals Ltd. (Unterach,. Austria). The surfactant, Tween 80, and cosurfactant, Span 20, were obtained from Al Shafei Medical and Scientific Equipment Est. (Jeddah, KSA). AGA oil was purchased from iHerb (http://sa.iherb.com) and CNAM oil was obtained from the Secret of Egypt (Sharm El Sheikh, Egypt). All the materials for tissue culture were purchased from UFC Biotechnology, Inc. (Jeddah, KSA). Cell counting kit-8 (CCK-8, Lot. No. LE612) was purchased from Dojindo Molecular Technologies (Kumamoto, Japan). Cell Death Detection Elisa^{Plus} (Lot. No. 19315700) was purchased from Roche (Mannheim, Germany). Annexin V-FITC/PI Apoptosis Detection Kit was purchased from MyBioSource (California, USA). 2',7'-dichlorofluorescein diacetate (DCFH-DA, Cat. No. 85155) was purchased from Cayman (Ann Arbor, USA). QCM™ 24-Well Collagen-Based Cell Invasion Assay (Cat. No. ECM 551) was purchased from Merck KGaA (Darmstadt, Germany).

Cell lines and cell culture

The human liver cancer cell lines, HepG2 and Huh7, were procured from America Type Tissue Culture Collection (Manassas, VA, USA). Cells were seeded in a 25 cm^2 cell culture flask containing Dulbecco's Modified Eagle's Medium (DMEM) supplemented with 10% (v/v) fetal bovine serum (FBS) and 1% (v/v) penicillin-streptomycin followed by incubation in 5% CO_2 95% humidified atmosphere incubator at 37°C. Cells were detached using 0.25% trypsin and resuspended in fresh media once every 48 h.

Formulation of AGA-CNAM and EPI-AGA-CNAM

Oil-in-water nanoemulsion (AGA-CNAM) was prepared by mixing the volume fractions (v/v) of 0.86 phosphate buffer (50 mM, pH 7), 0.1 surfactant mixture, and 0.02 of each AGA and CNAM oils. Then, the blend was sonicated in a sonicator (OMNI International, SONIC Ruptor 4000, Georgia, USA) with an amplitude of 40% for 15 min to get a clear and transparent solution. To neutralize the generated heat, the tube was kept in an ice bucket throughout the sonication period. EPI-AGA-CNAM was produced by directly solubilizing 29.40 µL of 2 mg/mL EPI in 970.60 µL of the AGA-CNAM solution. Then, serial dilutions of the stock solution were produced using culture media to prepare the required concentrations. It should be noted that the added amount of AGA-CNAM is the same as that added when mixing the EPI with AGA-CNAM.

Physical characterization

The Z-average diameter (nm), polydispersity index (PDI), and zeta potential (ZP) (mV) of AGA-CNAM and EPI-AGA-CNAM were measured by Malvern Zetasizer analyzer instrument at a scattering angle of 90° (Malvern Instruments Ltd., Malvern, UK). The experiment was performed 3 times at room temperature.

In vitro drug release

The drug release behavior of EPI and EPI-AGA-CNAM was measured by the dialysis bag diffusion technique. A 2 mL of 2 mg/mL of each sample was placed in the dialysis bag and immersed with 250 mL phosphate buffer (50 mM, pH 7). The released solution was kept at 37°C with stirring. At each period (0, 1, 2, 3, 4, 5, 6, 7, and 8 h), 2 mL of the sample was withdrawn and replaced with an equivalent volume of fresh medium. The absorbance of the collected samples was measured by the UV-visible spectrophotometer (Thermo Fisher Scientific, USA).

Cytotoxicity assay

The antiproliferative abilities of EPI, AGA-CNAM, and EPI-AGA-CNEM were evaluated by the Cell Counting Kit-8 (CCK-8) assay. Briefly, 100 µL of culture media containing 10,000 cells was plated in each well of 96-well plate and incubated overnight in 95% air and 5% humidified CO_2 at

37°C. Following cellular adherence, the old media were replaced with fresh media containing 100 µL of different concentrations of EPI, AGA-CNAM, and EPI-AGA-CNAM. After further incubation for up to 24 h, 5 µL of CCK-8 solution was added to each well and incubated for 3 h. Wells, included culture media, were considered negative control while culture media containing cells served as a positive control. The absorbance (A) was measured to determine the cellular proliferation at 450 nm in a multi-well ELISA plate reader (BioTek, US). The percentages of cellular proliferation were calculated according to the following equation:

$$\text{Cellular proliferation (\%)} = ((A_{\text{treated cells}} - A_{\text{negative cell}})/(A_{\text{positive cell}} - A_{\text{negative cell}})) \times 100$$

Morphological study

To determine the effects of EPI, AGA-CNAM, and EPI-AGA-CNAM on the morphology of the cells, both HepG2 and Huh7 cells (10,000) were suspended in DMEM containing 10% FBS, seeded in a 96-well plate, and incubated overnight in 95% air and 5% humidified CO_2 at 37°C for 24 h. After that, the original DMEM was replaced with fresh media containing 100 µL of the determined IC_{50} for the tested formulas and incubated for 24 h. After discarding the medium, cells were washed twice with 100 µL of PBS, fixed with 100 µL of 4% formaldehyde for 10 min, and stained with 5% Coomassie Blue. Finally, the stain solution was discarded, washed with 100 µL of tap water twice, and left to dry at room temperature. The changes in the cellular morphology were observed and photographed by an Olympus microscope (Olympus Corporation, Tokyo, Japan).

Annexin V-FITC/PI assay

HepG2 and Huh7 cells (2×10^5) were placed on a 6-well plate and incubated in 5% CO_2 incubator at 37°C for 24 h. Cells were treated with 100 µL of the IC_{50} for EPI, AGA-CNAM, and EPI-AGA-CNAM. After 24 h, cells were harvested and then washed 2 times with cold PBS. After centrifugation, the supernatant was discarded, and the pellets were resuspended in Annexin V-FITC/PI binding buffer and transferred into the flow cytometry tubes. Then, 5 µL of Annexin V-FITC and 5 µL of PI were added and left in the dark for 20 min at room temperature. Cells were analyzed on a flow cytometer using FACSDiva software (BD Biosciences, US).

DNA fragmentation assay

For the detection of apoptosis, the percentage of mono- and oligo-nucleosomes (DNA fragmentation (was carried out according to the protocol described in Cell Death Detection ELISA Kit^{Plus}. Cells (10,000) were cultured in a flat-bottomed 96-well plate containing 100 µL of growth media and were placed in a CO_2 incubator at 37°C for 24 h. Then, cells were harvested after the treatment for 24 h with 100 µL of the IC_{50} for EPI, AGA-CNAM, and EPI-AGA-CNAM. To eliminate the intact cell nuclei, cells were lysed in lysis buffer for 30 min and centrifuged at 200× *g* for 10 min. The supernatant (20 µL) with histone-linked DNA fragments was carefully applied on streptavidin-coated microplate well and incubated with immunoreagent (80 µL) with gentle shaking for 2 h. Thereafter, the wells were washed thrice and incubated for 20 min with a substrate provided by the kit's manufacturer. The color developed was quantified at 405 nm. The DNA fragmentation expressed as histone-associated mono- and oligo-nucleosomes released into the cytoplasm.

Reactive oxygen species (ROS) detection assay

The intracellular ROS production in response to EPI, AGA-CNAM, and EPI-AGA-CNAM treatments was determined using fluorescent probe 2',7'-dichlorofluorescein diacetate (DCFH-DA) which is an oxidation-sensitive fluorescence probe. DCFH-DA on enzymatic hydrolysis by intracellular esterases forms non-fluorescent DCF-H, which is subsequently oxidized to highly fluorescent DCF in the presence of ROS. Briefly, 100 µL culture media containing 10,000 cells was plated in each well of 96-well plate and incubated overnight in 95% air and 5% humidified CO_2 at 37°C. Then, cells were treated with 100 µL of the IC_{50} for EPI, AGA-CNAM, and EPI-AGA-CNAM. After 24 h of treatment, cells were washed with PBS and subsequently incubated with 5 µL DCFH-DA dye for 30 min. Fluorescence was monitored at an excitation wavelength of 485 nm and an emission wavelength of 528 nm using a fluorescence microplate reader (BioTek, US).

Invasion assay

Trans-well invasion assay was performed to determine the effect of EPI, AGA-CNAM, and EPI-AGA-CNAM treatment on cancer cell motility *in vitro* using QCM™ 24-Well Collagen-Based Cell Invasion Assay. Cells (10,000) were cultured in a flat-bottomed 96-well plate containing 100 µL of growth media and were placed in a CO_2 incubator for 24 h at 37°C. Then, cells were treated with 100 µL of the IC_{50} for each tested formula and incubated for 24 h. After that, cells were harvested, resuspended in serum-free media, and seeded into the upper chambers insert with the 8 µm pore of 24-well plate while the lower chambers were filled with 500 µL serum-free medium. After a 24 h incubation period at 37°C, non-invading cells were removed while the invaded cells were fixed, stained with 5% Coomassie Blue, eluted with 10% acetic acid, and photographed using a light microscope (Olympus Corporation, Tokyo, Japan). Absorbance was measured at 560 nm using a microplate reader (BioTek, US).

Statistical analysis

MegaStat (version 10.3, Butler University, Indianapolis, IN) software was used in all statistical analyses performed in this study. Statistical comparisons were conducted using

one-way analysis of variance (ANOVA). The independent samples *t*-test was used to compare two independent groups. All results have been presented as mean ± standard deviation (SD). The variations between the samples were considered when $P < 0.05$.

RESULTS

Physical characterizations of produced nanoemulsion formulas

According to the Zetasizer measurements summarized in Table 1, the mean size of the dispersed nanosuspensions for AGA-CNAM was manifestly enlarged when loaded with EPI. In fact, the distributions of the nanodroplet sizes for both AGA-CNAM and EPI-AGA-CNAM were homogeneous since the values of PDI were smaller than 0.250. Although the surface charge of the nanodroplets expressed as ZP for both AGA-CNAM and EPI-AGA-CNAM was negative, the magnitudes of ZP for both formulas were markedly different.

In vitro drug release

The *in vitro* drug release profiles for both EPI and EPI-AGA-CNAM were assessed, as shown in Figure 1. The released cumulative amount of EPI-AGA-CNAM was higher than EPI at a different period ($P < 0.05$). Interestingly, both EPI-AGA-CNAM and EPI exhibited sustained release profiles within 24 h with a cumulative drug release percentages of 98.7 and 91.4, respectively.

Cytotoxicity assay

The cytotoxicity of EPI, AGA-CNAM, and EPI-AGA-CNAM was evaluated in HepG2 and Huh7 cell lines using CCK-8 assay. According to Figure 2, both HCC cells responded to the cytotoxic effects of the tested formulas in a dose-dependent manner. When HepG2 and Huh7 cells were treated with different concentrations (0.1–5.00 μM) of AGA-CNAM and EPI-AGA-CNAM for 24 h, the percentages of cellular proliferation were significantly diminished when compared to EPI at the same concentration ($P < 0.001$). According to the determined IC_{50} values illustrated in Table 2, there were no significant differences between both cells in their response to each formula ($P > 0.05$). However, both cells were enormously

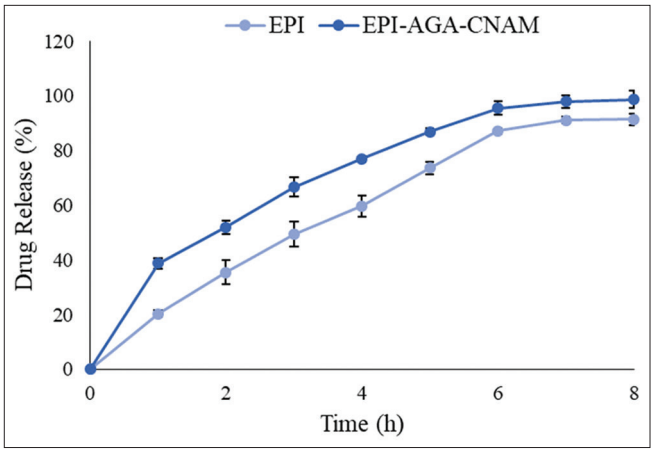

Figure 1: The *in vitro* cumulative drug release profile of EPI and EPI-AGA-CNAM in phosphate buffer (50 mM, pH 7).The study was carried up to 8 h. The results were expressed as mean ± SD for three determinations

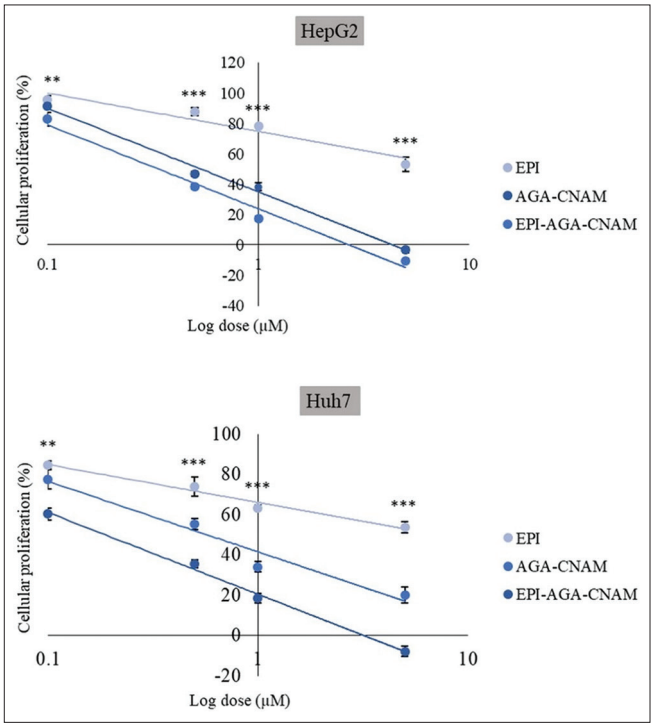

Figure 2: Dose–response effect of EPI, AGA-CNAM, and EPI-AGA-CNAM in HepG2 and Huh7 cells after 24 h exposure using CCK-8 assay. Data are expressed as mean ± SD for three determinations. The considerable differences between the groups, determined by one-way ANOVA, were classified to highly (**$P < 0.01$) and very highly (***$P < 0.001$)

Table 1: Zetasizer measurements of the produced formulas

Tested formula	Z-average diameter (nm)	PDI	Zeta potential (mV)
AGA-CNAM	17.10±1.25	0.073±0.02	−2.01±0.05
EPI-AGA-CNAM	109.90±2.97	0.027±0.03	−2.98±0.22
P-value	<0.001 v.HS	>0.05 NS	<0.01 HS

Data were presented as the mean±SD for three determinations. PDI: Polydispersity index. The differences between AGA-CNAM and EPI-AGA-CNAM were performed with the independent sample *t*-test and expressed as v.HS: Very highly significant, HS: Highly significant, and NS: No significant

Table 2: IC_{50} values of the tested formulas when subjected to HepG2 and Huh7 cell lines for 24 h

	IC_{50} (μM)	
Treatments	**HepG2**	**Huh7**
EPI	5.25±1.12	7.40±1.32
AGA-CNAM	0.53±0.16	0.47±0. 12
EPI-AGA-CNAM	0.32±0.15	0.20±0.11

Data were presented as the mean±SD for three determinations. The differences between HepG2 and Huh7 at each individual formula were performed with the independent sample *t*-test and expressed as no significant when $P>0.05$

sensitive to AGA-CNAM and EPI-AGA-CNAM treatments relative to EPI treatment ($P < 0.001$) which indicates that the nanoemulsion formulas have stronger cytotoxic activity against HCC cells than free EPI.

Visualization of cellular morphology

The HepG2 and Huh7 cell morphologies were observed and captured on treatment for 24 h with IC_{50} doses for the investigated formulas using a light microscope. In the control group, despite the duration of treatment with only culture media, the untreated cells contained the formation of the fusion colony cells which maintained most of their morphological features, as shown in Figure 3. In contrast, cells exposed to the treatment with the IC_{50} doses of AGA-CNAM and EPI-AGA-CNAM had changed morphologically since the membrane blebbing, cell shrinkage, and pyknosis were seen indicating that the cells were enduring apoptosis. Interestingly, cells treated with EPI-AGA-CNAM were diminished and exhibited more signs for late apoptosis as chromatin segmentation and release of apoptotic bodies were seen.

Annexin V-FITC/PI assay

Annexin V-FITC/PI double staining was applied to evaluate the apoptosis on treatment with the IC_{50} doses of EPI, AGA-CNAM, and EPI-AGA-CNAM for 24 h against HepG2 and Huh7 cells using flow cytometry. As shown in Figure 4 a and b, EPI-AGA-CNAM induced more apoptosis in early stages on both HepG2 and Huh7 cells ($P < 0.001$) compared with free EPI. The Annexin V intensity levels of the HepG2 cells was significantly higher than that of Huh7 cells in response to all investigated formulas ($P < 0.001$). Figure 4c shows that EPI-AGA-CNAM induced higher Annexin V/PI levels (35.40 ± 1.97) in HepG2 cells in comparison to EPI (26.60 ± 0.36). However, in Huh7 cells, a high level of Annexin V/PI was observed on treatment with free EPI.

DNA fragmentation assay

Apoptosis induction was verified by the assessment of the intracellular level of histone-associated mono- and oligo-nucleosomes. What can be clearly seen in Figure 5 is the large level of DNA apoptotic degradation observed in HepG2 and Huh7 cells in response to EPI-AGA-CNAM which were higher than the corresponding controls by 7.4- and 3.5-folds, respectively ($P < 0.001$). All the investigated formulas have more apoptotic effects on HepG2 cells than Huh7 cells as the fraction of the mono- and oligo-nucleosomes was augmented in HepG2-treated cells ($P < 0.001$).

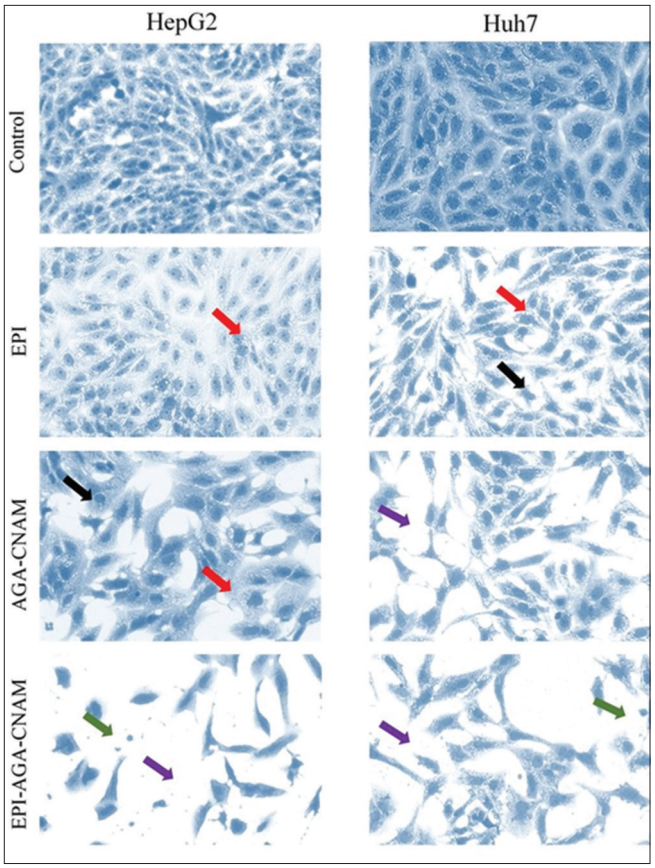

Figure 3: Light microscopy images displaying morphological changes induced in HepG2 and Huh7 cells after treated for 24 h with the IC_{50} of EPI, AGA-CNAM, and EPI-AGA-CNAM and stained with 5% Coomassie Blue. Images were magnified at 40×. Signs of apoptosis are represented by the red arrows (membrane blebbing), black arrows (cell shrinkage), purple arrows (intercellular space), and green arrows (apoptotic bodies)

ROS detection assay

As shown in Figure 6, the DCF fluorescence intensities were significantly increased in HepG2 and Huh7 cells following exposure to the IC_{50} doses of AGA-CNAM (69.89 ± 1.84 and 62.25 ± 3.50, respectively) and EPI-AGA-CNAM (84.56 ± 2.21 and 78.01 ± 3.30, respectively) compared to the group treated with the IC_{50} of EPI (13.6 ± 3.77 and 11.67 ± 4.28, respectively). Moreover, the sensitivity of the fluorescence probe in HepG2 to AGA-CNAM and EPI-AGA-CNAM was significantly higher than that of Huh7 indicating higher amounts of ROS formation in the cells.

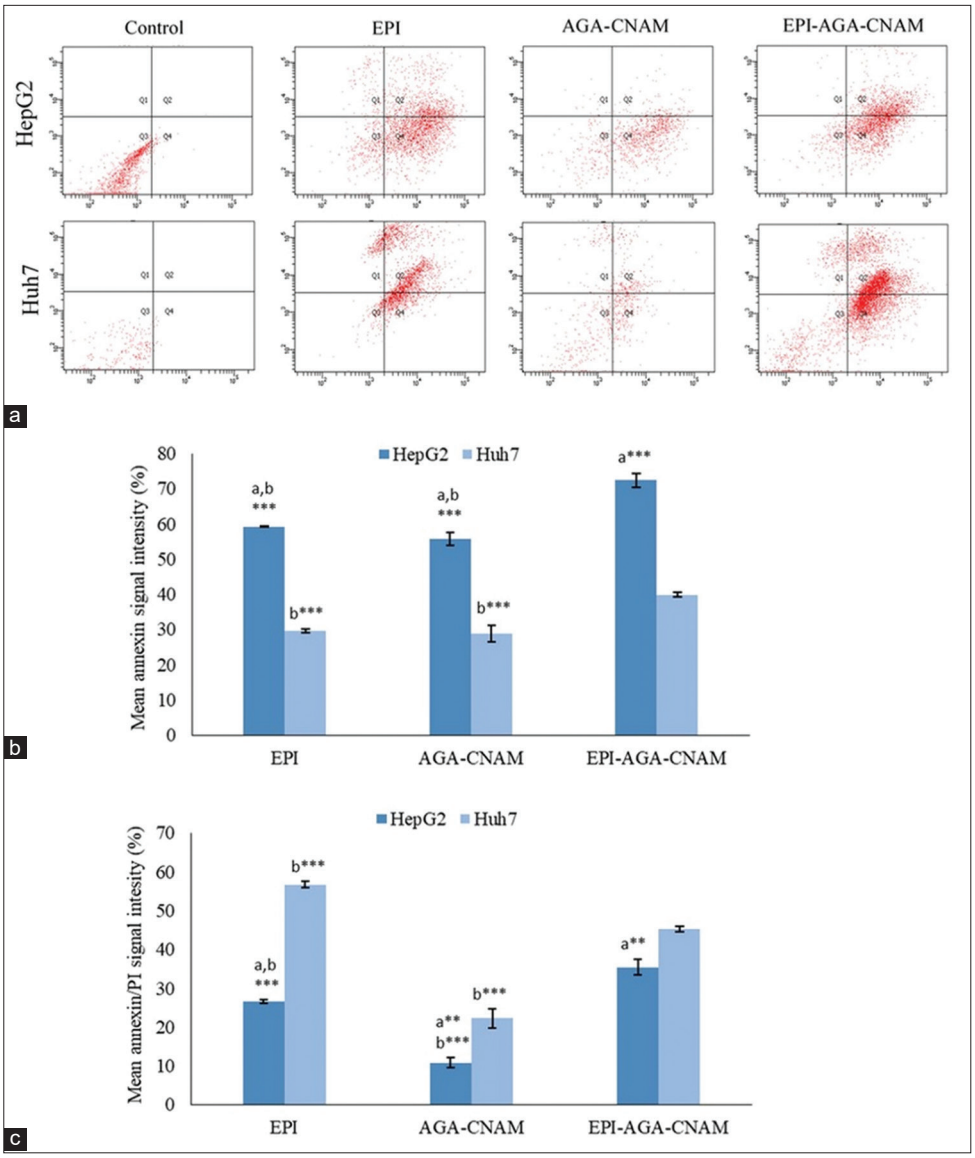

Figure 4: Annexin V-FITC/PI double staining analysis of apoptosis in HepG2 and Huh7 cells treated with the IC_{50} of EPI, AGA-CNAM, and EPI-AGA-CNAM for 24 h. (a) Representative flow cytometry plots of the untreated (control) and treated HepG2 and Huh7 cells, stained with Annexin V-FITC/PI. (b) The percentages of early apoptotic cells indicated by the percentages of mean Annexin V signal intensity versus the tested treatment. (c) The percentages of late apoptotic cells indicated by the percentages of the mean Annexin V/PI signal intensity. The symbol ([a]) represents the differences between HepG2 and Huh7 subjected to the tested formulas. The symbol ([b]) represents the differences between the tested formulas and EPI-AGA-CNAM in the same cell line. The considerable differences between the groups, determined by one-way ANOVA, were classified to highly (**$P < 0.01$) and very highly (***$P < 0.001$)

Invasion assay

According to the trans-well assay, the number of HepG2 and Huh7cells that accomplished invasion was markedly reduced on treatment with the IC_{50} of EPI-AGA-CANM when compared to the other treated cells, as shown in Figure 7a and b. In particular, the invasive potential of HepG2 and Huh7 cells on treatment with EPI-AGA-CNAM was reduced to 39% in comparison to the treatment with EPI alone (55.58% and 63.35%, respectively). There were no significant differences between the two cell lines on treatment with EPI-AGA-CNAM. In contrast, HepG2 cells were more sensitive to AGA-CNAM than Huh7 cells ($P < 0.05$).

DISCUSSION

HCC is the fifth common cancer in humans and one of the most common forms of liver cancer. The HCC exhibits poor response to conventional treatments and presents serious resistance to classical chemotherapy. In this regard, EPI is reported to possess excellent anticancer efficacy in many cancers including liver cancer. However, clinical applications of EPI have been limited by serious health problems and lack of its ability to accumulate in the cancer tissues.[15] Therefore, the current study estimates the nanocarrier-mediated drug delivery of this drug. AGA-CNAM was prepared with the

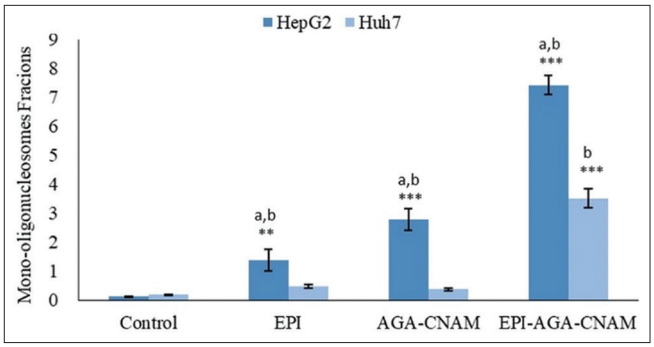

Figure 5: The apoptosis assessment indicated by the mono- and oligo-nucleosomes fractions, measured by the Cell Death Detection ELISA assay, in HepG2 and Huh7 cells incubated for 24 h with the IC_{50} of EPI, AGA-CNAM, or EPI-AGA-CNAM. Data were expressed as mean ± SD for three determinations. The symbol ([a]) represents the differences between HepG2 and Huh7 subjected to the tested formulas. The symbol ([b]) represents the differences between the tested formulas and EPI-AGA-CNAM in the same cell line. The considerable differences between the groups, determined by one-way ANOVA, were classified to highly (**$P < 0.01$) and very highly (***$P < 0.001$)

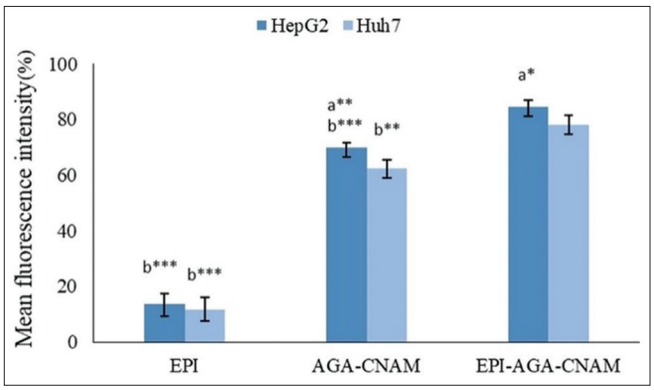

Figure 6: The mean fluorescence intensity of HepG2 and Huh7 cells undergoing induction of ROS using DCFH-DA (an oxidant-sensitive fluorescent probe) in response to the IC_{50} of EPI, AGA-CNAM, or EPI-AGA-CNAM after 24 h. Data were expressed as mean ± SD for three determinations. The symbol ([a]) represents the differences between HepG2 and Huh7 subjected to the tested formulas. The symbol ([b]) represents the differences between the tested formulas and EPI-AGA-CNAM in the same cell line. The considerable differences between the groups, determined by one-way ANOVA, were classified to regular (*$P < 0.05$), highly (**$P < 0.01$), and very highly (***$P < 0.001$)

aim to improve the anticancer efficacy and targeting the delivery of EPI.

The mean particle size was determined using the dynamic light scattering. EPI-AGA-CNAM was larger than blank AGA-CNAM which indicates the presence of EPI inside the core of the nanosuspension. In this research, both AGA-CNAM and EPI-AGA-CNAM showed a relatively narrow size distribution (PDI < 0.10), which makes them particularly favorable for use in the drug delivery system.[6]

CCK-8 analysis revealed that the blank AGA-CNAM and EPI-AGA-CNAM have greater inhibition effect on the HCC cell proliferation than the EPI effect. Consistently, the IC_{50} values of EPI-AGA-CNAM on HepG2 and Huh7 were markedly lower than the values of EPI. Similar to our findings, the previous reports revealed that the antiproliferative activities of EPI-loaded nanoparticles subjected to various cancer cells were enhanced when compared to the free EPI.[3,15] Furthermore, cotreatment of essential oils and conventional chemotherapeutic agents had resulted in the improvement of the efficacy of these compounds through a synergistic effect against various cancer cells.[16-20]

To explore the cause of cell death in HepG2 and Huh7, cells were stained with Coomassie Blue dye and Annexin V-FITC/PI. Moreover, to confirm the ability of investigated formulas to induce apoptosis, DNA fragmentation assay was utilized. The results exhibited that EPI-AGA-CNAM induced more apoptosis on the cells when compared with free EPI. In fact, HepG2 cells endured more apoptosis features than Huh7 cells. The superior cytotoxic effect of EPI-AGA-CNAM may be attributed to the small size of the nanoformulation, which was <200 nm, resulting in high cellular uptake and accumulation of the high amount of anticancer drug within the tumor cells and enhanced permeation and retention (EPR) effect.[21,22] Furthermore, the cytotoxic effect of the free AGA-CNAM may be due to the incorporation of essential oils with emulsifying agents which lead to an increase in the permeability of formula and affecting the cell membrane of the cancer cell.

Although nanoparticles were generally reported to be inducer for ROS, cancer cotreatment between nanomaterials induced oxidative stress and chemotherapeutic agents was infrequently reported. Intracellular ROS production was evaluated by DCFH-DA staining. In our study, EPI-AGA-CNAM at its IC_{50} doses exhibited a drastically increased DCF fluorescence intensity levels in HepG2 and Huh7 cells. A similar result was recently reported that the hydrophobic GNPs increased the sensitivity of cancer cells to paclitaxel (PTX) through the induction of oxidative stress.[23] Furthermore, recent reports stated that different types of nanoparticles induce ROS generations.[23,24] Nanoparticles may interact with biomolecules through specific and non-specific interactions and induce oxidative stress in human cells through different pathways.[25] Once the nanoparticles diffuse into the human body, the overproduction of ROS stimulates the oxidative stress which leads to serious incidents of lipid peroxidation, apoptosis, and DNA breakdown.[26]

According to the trans-well assay, EPI-AGA-CNAM inhibited the invasiveness of HepG2 and Huh7 cells to a greater degree than free EPI which implies that the combined delivery of EPI and AGA-CNAM made an important impact on the metastatic ability of HepG2 and Huh7 cells. Likewise, loading the PTX and siRNA on poly(β-amino ester) nanoparticles had impeded the metastasis in breast cancer.[27]

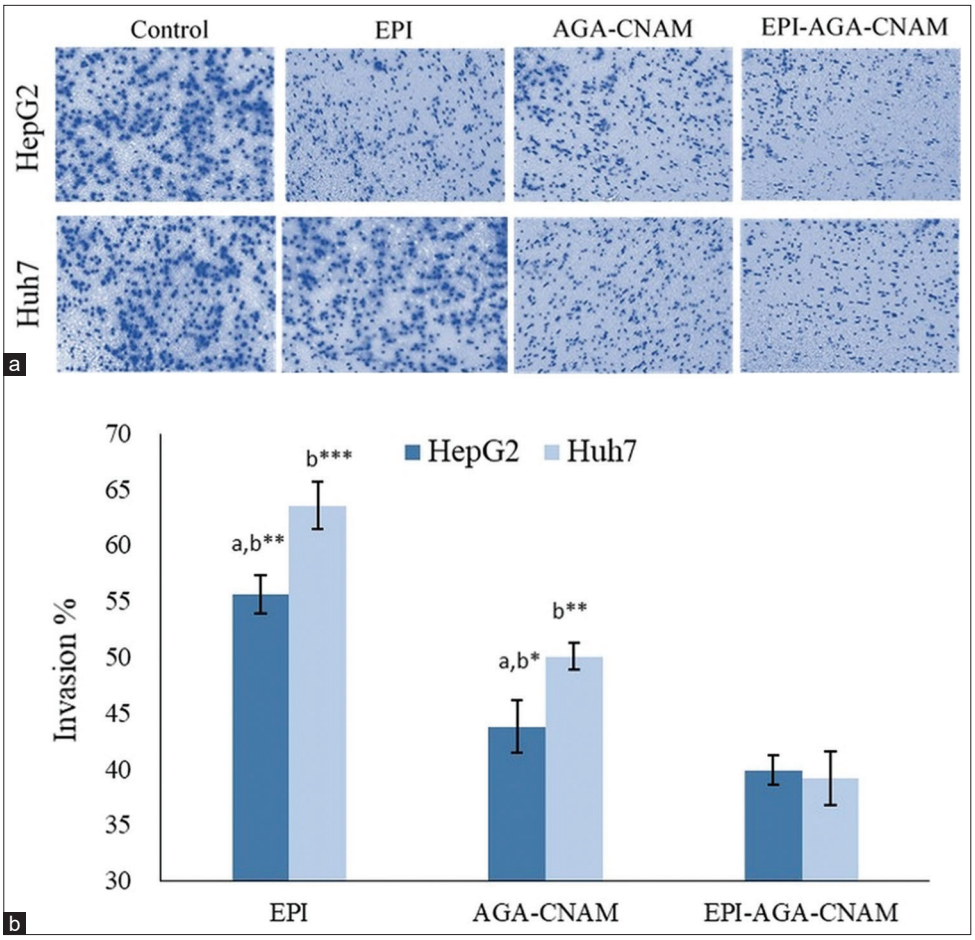

Figure 7: Invasion assay performed in HepG2 and Huh7 cell lines was detected by trans-well assay following 24 h treatment with the IC_{50} of EPI, AGA-CNAM, or EPI-AGA-CNAM. (a) Light microscopy images of the invaded cells (×20). (b) The percentages of the invaded cells relative to the control. Data were expressed as mean ± SD for three determinations. The symbol ([a]) represents the differences between HepG2 and Huh7 subjected to the tested formulas. The symbol ([b]) represents the differences between the tested formulas and EPI-AGA-CNAM in the same cell line. The considerable differences between the groups, determined by one-way ANOVA, were classified to regular (*$P < 0.05$), highly (**$P < 0.01$), and very highly (***$P < 0.001$)

CONCLUSION

EPI-AGA-CNAM exhibited superior cytotoxic and apoptotic effects on HepG2 and Huh7 when compared with the free EPI. EPI-AGA-CNAM exerts its cytotoxicity through the generation of ROS, which subsequently induces apoptotic death in liver cancer cells and reduces their invasion properties. Hence, nanoemulsion based on essential oils provides a promising potential for drug delivery.

REFERENCES

1. Wang SB, Ma YY, Chen XY, Zhao YY, Mou XZ. Ceramide-graphene oxide nanoparticles enhance cytotoxicity and decrease hcc xenograft development: A novel approach for targeted cancer therapy. Front Pharmacol 2019;10:69.
2. Wang X, Zhang H, Chen X. Drug resistance and combating drug resistance in cancer. Cancer Drug Resist 2019;2:141-60.
3. Chen X, Han W, Zhao X, Tang W, Wang F. Epirubicin-loaded marine carrageenan oligosaccharide capped gold nanoparticle system for pH-triggered anticancer drug release. Sci Rep 2019;9:6754.
4. Jalalian SH, Ramezani M, Abnous K, Taghdisi SM. Targeted co-delivery of epirubicin and NAS-24 aptamer to cancer cells using selenium nanoparticles for enhancing tumor response *in vitro* and *in vivo*. Cancer Lett 2018;416:87-93.
5. Tao W, Ji X, Zhu X, Li L, Wang J, Zhang Y, *et al*. Two-dimensional antimonene-based photonic nanomedicine for cancer theranostics. Adv Mater 2018;30:e1802061.
6. Wu B, Liang Y, Tan Y, Xie C, Shen J, Zhang M, *et al*. Genistein-loaded nanoparticles of star-shaped diblock copolymer mannitol-core PLGA-TPGS for the treatment of liver cancer. Mater Sci Eng C Mater Biol Appl 2016;59:792-800.
7. Takemae K, Okamoto J, Horise Y, Masamune K, Muragaki Y. Function of epirubicin-conjugated polymeric micelles in sonodynamic therapy. Front Pharmacol 2019;10:546.

8. Liu L, Mu LM, Yan Y, Wu JS, Hu YJ, Bu YZ, *et al*. The use of functional epirubicin liposomes to induce programmed death in refractory breast cancer. Int J Nanomedicine 2017;12:4163-76.
9. Suo N, Wang M, Jin Y, Ding J, Gao X, Sun X, *et al*. Magnetic multiwalled carbon nanotubes with controlled release of epirubicin: An intravesical instillation system for bladder cancer. Int J Nanomedicine 2019;14:1241-54.
10. Tariq M, Alam MA, Singh AT, Panda AK, Talegaonkar S. Improved oral efficacy of epirubicin through polymeric nanoparticles: Pharmacodynamic and toxicological investigations. Drug Deliv 2016;23:2990-7.
11. Arbain NH, Basri M, Salim N, Wui W, Rahman MA. Development and characterization of aerosol nanoemulsion system encapsulating low water soluble quercetin for lung cancer treatment. Mater Today 2018;5:S137-42.
12. Thompson M, Schmelz EM, Bickford L. Anti-cancer properties of cinnamon oil and its active component, trans-cinnamaldehyde. J Nutr Food Sci 2019;9:1000750.
13. Yang XQ, Zheng H, Ye Q, Li RY, Chen Y. Essential oil of cinnamon exerts anti-cancer activity against head and neck squamous cell carcinoma via attenuating epidermal growth factor receptor-tyrosine kinase. J BUON 2015;20:1518-25.
14. Yang CC, Hung CF, Chen BH. Preparation of coffee oil-algae oil-based nanoemulsions and the study of their inhibition effect on UVA-induced skin damage in mice and melanoma cell growth. Int J Nanomedicine 2017;12:6559-80.
15. Di-Wen S, Pan GZ, Hao L, Zhang J, Xue QZ, Wang P, *et al*. Improved antitumor activity of epirubicin-loaded CXCR4-targeted polymeric nanoparticles in liver cancers. Int J Pharm 2016;500:54-61.
16. Alkhatib MH, AlMotwaa SM, Alkreathy HM. Incorporation of ifosfamide into various essential oils-based nanoemulsions ameliorates its apoptotic effect in the cancers cells. Sci Rep 2019;9:695.
17. Alkhatib MH, Al-Otaibi WA, Wali AN. Antineoplastic activity of mitomycin C formulated in nanoemulsions-based essential oils on HeLa cervical cancer cells. Chem Biol Interact 2018;291:72-80.
18. Al-Otaibi WA, Alkhatib MH, Wali AN. Evaluation of antitumor activity and hepatoprotective effect of mitomycin C solubilized in chamomile oil nanoemulsion. Anticancer Agents Med Chem 2019;19:1232-42.
19. Alkhatib MH, Albishi HM. *In vitro* evaluation of antitumor activity of doxorubicin-loaded nanoemulsion in MCF-7 human breast cancer cells. J Nanopart Res 2013;15:1489.
20. Almotwaa SM, Alkhatib MH, Alkreathy HM. Nanoemulsion-based camphor oil carrying ifosfamide: Preparation, characterization, and *in vitro* evaluation in cancer cells. Int J Pharm Sci Res 2019;10:2018-26.
21. Golombek SK, May JN, Theek B, Appold L, Drude N, Kiessling F, *et al*. Tumor targeting via EPR: Strategies to enhance patient responses. Adv Drug Deliv Rev 2018;130:17-38.
22. Chitgupi U, Qin Y, Lovell JF. Targeted nanomaterials for phototherapy. Nanotheranostics 2017;1:38-58.
23. Sun H, Liu Y, Bai X, Zhou X, Zhou H, Liu S, *et al*. Induction of oxidative stress and sensitization of cancer cells to paclitaxel by gold nanoparticles with different charge densities and hydrophobicities. J Mater Chem B 2018;6:1633-9.
24. Martínez-Torres AC, Zarate-Triviño DG, Lorenzo-Anota HY, Ávila-Ávila A, Rodríguez-Abrego C, Rodríguez-Padilla C. Chitosan gold nanoparticles induce cell death in HeLa and MCF-7 cells through reactive oxygen species production. Int J Nanomedicine 2018;13:3235-50.
25. Kim YJ, Yu M, Park HO, Yang SI. Comparative study of cytotoxicity, oxidative stress and genotoxicity induced by silica nanomaterials in human neuronal cell line. Mol Cell Toxicol 2010;6:336-43.
26. Phaniendra A, Jestadi DB, Periyasamy L. Free radicals: Properties, sources, targets, and their implication in various diseases. Indian J Clin Biochem 2015;30:11-26.
27. Tang S, Yin Q, Su J, Sun H, Meng Q, Chen Y, *et al*. Inhibition of metastasis and growth of breast cancer by pH-sensitive poly (β-amino ester) nanoparticles co-delivering two siRNA and paclitaxel. Biomaterials 2015;48:1-5.

Source of Support: Nil. **Conflicts of Interest:** None declared.